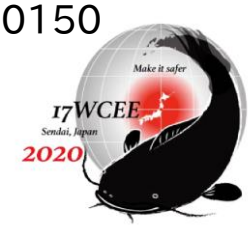

17th World Conference on Earthquake Engineering, 17WCEE
Sendai, Japan - September 13th to 18th 2020

REPAIRING AND STRENGTHENING NON-DUCTILE REINFORCED CONCRETE COLUMNS TO RESIST SEISMIC DEMANDS

J. Monical[(1)], K. Skillen[(2)], P. Shah[(3)], S. Pujol[(4)]

[(1)] *Graduate Student, Purdue University, jmonica@purdue.edu*
[(2)] *Research Engineer, Purdue University, kskillen@purdue.edu*
[(3)] *Graduate Student, Purdue University, shah151@purdue.edu*
[(4)] *Professor, University of Canterbury, santiago.pujol@canterbury.ac.nz*

Abstract

This study focuses on a method for cost-effective repair and strengthening of non-ductile reinforced concrete columns vulnerable to shear induced by earthquakes. In this method, external post-tensioned “clamps” are installed along the height of the column. Each clamp consists of threaded rods, nuts, and structural steel angles. The clamps increase the drift capacity of the column by providing active confinement not requiring large deformations of the concrete core to become effective. The clamps can be fabricated and installed with minimal expertise using widely available and inexpensive materials and tools.

Two series of tests were conducted on a single small-scale reinforced concrete frame on an earthquake simulator. The first series of tests was conducted on the bare frame and before repairs. After several runs of increasing intensity, the bare frame – that had column ties spaced at a distance equal to the column effective depth d – was judged to be close to shear failure associated with large inclined cracks that formed within spaces between ties. Testing was suspended and the clamps were applied to the damaged frame. Runs of increasing intensities followed by runs of decreasing intensities were carried out for the frame with clamps. The repaired frame sustained 22 motions without a perceptible loss in its ability to resist seismic demands. Remarkably, the peak drifts reached in the tests of the repaired structure were similar to those of the bare frame even after tens of runs inducing large drifts. In addition, drift was observed to be nearly proportional to peak base velocity. These observations have two implications:

1. The external post-tensioned clamps used were an effective means to maintain the strength of the frame with increasing drift demands.
2. In well confined columns with adequate anchorage, peak drift was not sensitive to loading history.

Keywords: reinforced concrete; non-ductile; seismic; shear strengthening; drift

1. Introduction

Scores of RC buildings built with inadequate seismic detailing have collapsed in the past 50 years. More are bound to collapse in the next earthquake if nothing is done to strengthen older, vulnerable buildings. Many effective strengthening methods are currently used. The most commonly used methods such as fiber reinforced polymer (FRP) wrapping and steel jacketing require expert installation involving gluing or welding. Also, the necessary materials (e.g., FRP fabric and epoxy), tools, and workmanship are expensive and not widely available. Stiffening of buildings with shear walls is an option that reduces seismic drift demand but may disrupt the use of the building and requires additional design. In this investigation, a post-tensioned transverse reinforcement device that can be easily sized, fabricated, and installed is proposed. It does not reduce drift demand but it does increase drift capacity.

The post-tensioned transverse reinforcement used in this study was previously investigated by Skillen [1]. Skillen used post-tensioned transverse reinforcement to investigate the effects of strength and deformability of full-scale reinforced concrete columns with transverse reinforcement detailing similar to that of columns tested by Sezen [2]. Skillen constructed and tested two reinforced concrete columns, one with post-tensioned transverse reinforcement and one without. The post-tensioned transverse reinforcement was installed along the height of the column prior to testing. Both columns developed their lateral strengths at a drift ratio of approximately 1%, but the bare column failed in shear and lost its axial capacity at a drift ratio of 1.5%. The column with post-tensioned transverse reinforcement did not fail in shear and reached drift ratios exceeding 7% while maintaining 75% of its lateral strength. The device was effective in preventing a shear failure and provided sufficient deformation capacity for columns in buildings subjected to strong ground motions.

A similar device referred to as a prestressed external hoop was tested by Yamakawa et al. [3]. Yamakawa subjected 31 reinforced concrete columns with light transverse reinforcement to cyclic loading with a constant axial load of approximately 20% of the axial capacity. Some columns were tested with external hoops installed along the height of columns while others had no external hoops. The hoops were prestressed to the column face using threaded rods. Test results showed that adding prestressing improved deformability of columns and prevented shear failures in comparison to columns without external hoops. Columns with external hoops reached drift ratios at least twice as large as columns without hoops.

In comparison to the device used by Yamakawa, the device used by Skillen was a simpler design, less expensive to fabricate and easier to install. Therefore, the device used by Skillen was selected in this experimental program.

2. Experimental Program

2.1 Test specimens

A small-scale reinforced concrete frame was tested in its strong direction on a single degree-of-freedom earthquake simulator (Fig. 1, 2). Two series of tests were conducted using the same reinforced concrete frame. In series one, the bare frame was subjected to ground motions of increasing intensities until it was judged that the frame was close to shear failure. Series one was completed with two additional repetitions at the 40% motion. Testing was suspended and post-tensioned transverse reinforcement, or clamps, was installed along the height of the columns of the damaged frame prior to additional testing. In series two, the repaired frame was subjected to a set of increasing ground motions. After the frame with clamps was subjected to two runs at the 100% motion, the frame was subjected to ground motions of decreasing intensities. Runs of decreasing intensities were used to observe the response of structures to lower-intensity ground motions after being subjected to strong ground motions.

The test frame had a column centerline-to-centerline distance of 6 ft. and a column clear height of 40 in. (Fig. 3). The dimensions of the columns were 8 in. by 8 in. with four #5 longitudinal bars with a measured yield stress of 65 ksi. Effective depth *d* was 6 in. The measured concrete compressive strength was 3800 psi. The transverse reinforcement in the columns represented details common in older construction and consisted

of #3 ties spaced at *d* with a measured yield stress of 70 ksi. The resulting transverse reinforcement ratio of 0.5% was larger than typical ratios in vulnerable buildings. Nevertheless, the effects of the wide tie spacing were assumed to dominate and offset the effects of mentioned ratio. The cross-sections of the column and beam are shown in Fig. 3. The reinforcement details are shown in Fig. 4.

The layout of the clamps applied along the height of the columns is shown in Fig. 5. The top and bottom clamps were placed at 2 in. from the beam-column joint. This location coincided with the top and bottom ties cast within the column. The next three clamps at each end were spaced at *d*/2. The middle two clamps were spaced at *d*. The cross-section of the clamp assembly is shown in Fig. 6. The threaded rods used in the clamps were stressed to approximately 40 ksi for an effective confining stress of 470 psi at column ends and 230 psi at mid-height. The confining stress at column ends (470 psi) was comparable to the maximum nominal shear stress expected in each column.

2.2 Test setup and instrumentation

An isometric of the test setup is shown in Fig. 1. The simulator moved the base of the test specimen in the direction of the longitudinal axis of the frame. Details of the simulator are provided in Sozen [4]. The simulator was operated using a displacement control procedure. A 14 ft. x 4 ft. x 5 ft. (L x W x H) 42 kip concrete block was suspended in the air by an overhead crane positioned 35 ft. above the top of the block. The center of mass of the block and the top beam were aligned. The block was used to provide additional mass to the system so that the response of the frame became nonlinear before reaching the limits of the simulator.

A double swivel connection was used to connect the suspended block to the top beam to prevent the transfer of bending moment to the top beam. After the first four runs, it was determined that the double swivel connection was inadequate in preventing play between the mass and the frame. For subsequent runs, the connection was improved using mechanical fasteners that prevented play.

The suspended block was connected to two MC18x58 steel channels confining the top beam of the frame with a clamping force of approximately 300 kip. A layer of gypsum cement was applied between the steel channel and concrete of the top beam to ensure uniform contact. Adjustable bolts bore on 0.25 in. thick steel plates attached to the top RC beam and angles bolted to channels at both ends of the specimen to prevent channels from sliding relative to beam (Fig. 1).

The base of the frame was clamped to the earthquake simulator using steel channels and steel angles. The total clamping force was approximately 220 kip. Four hollow structural sections (HSS) were used to prevent out-of-plane displacement of the mass. Each HSS was clamped to a concrete block that was post-tensioned to the floor. Teflon pads and stainless-steel plates were installed between the HSS and the block to reduce friction.

A load cell was placed in series with the suspended block and frame to measure lateral force. A total of four accelerometers were positioned on top of the bottom and top beam at the northeast and southwest corners. Four accelerometers were attached to the suspended concrete block. Data from the accelerometers were used to measure base motion parameters and lateral force. Three linear variable differential transformers (LVDTs) connected to the top of the bottom beam, and bottom and top of the top beam on the north side of the frame were used to measure the relative displacement of the frame with respect to the simulator platform.

The initial, uncracked period of the frame with additional mass was calculated to be 0.11 s. From free-vibration tests, the initial period of the frame without additional mass was measured to be 0.04 s. Using the results from free-vibration tests, the initial period of the frame with additional mass was inferred to be 0.15 s. The nominal strength of the frame was calculated to be 22 kip.

2.3 Input ground motion

The simulated ground motion was modeled after the north-south component of the 1940 El Centro earthquake. The record was obtained from PEER NGA West-2 ground motion database [5] who report to have corrected or modified it to meet expectations about credible ground displacement. To meet the operating limits of the earthquake simulator and to ensure nonlinear response of the frame, the time scale of the ground motion was

scaled down by a factor of 2 and the amplitude was scaled up by 1.9. The resulting scaled ground motion at 100% intensity had a peak acceleration (PGA) of 0.53 g, peak velocity (PGV) of 11.6 in./s and peak displacement (PGD) of 1.62 in. For intensities less than the 100% motion, the expected ground motions were linearly scaled in amplitude with the percentages listed in column 2 of Tables 1 and 2.

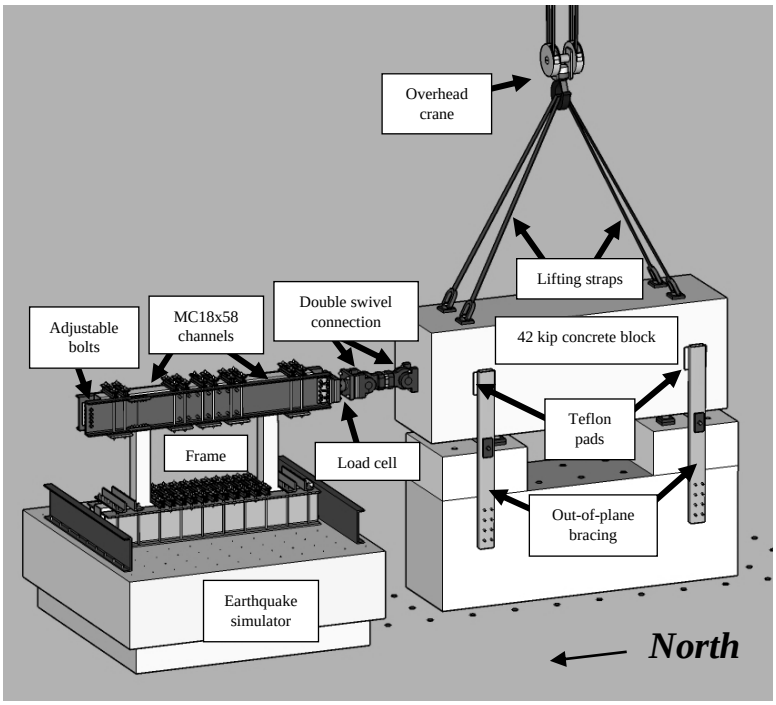

Fig. 1 – Isometric of test setup

(a)

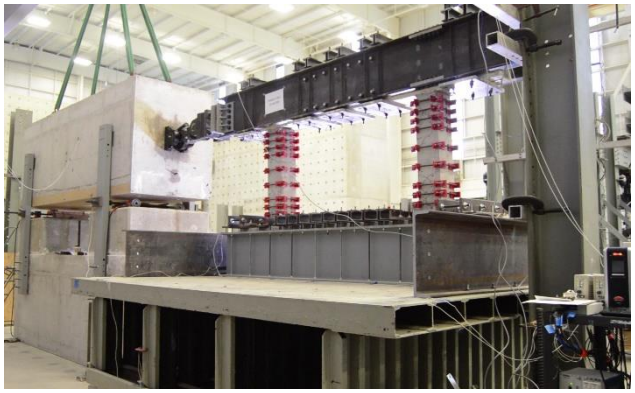

(b)

Fig. 2 – Photograph of test setup of (a) bare frame, (b) frame with clamps

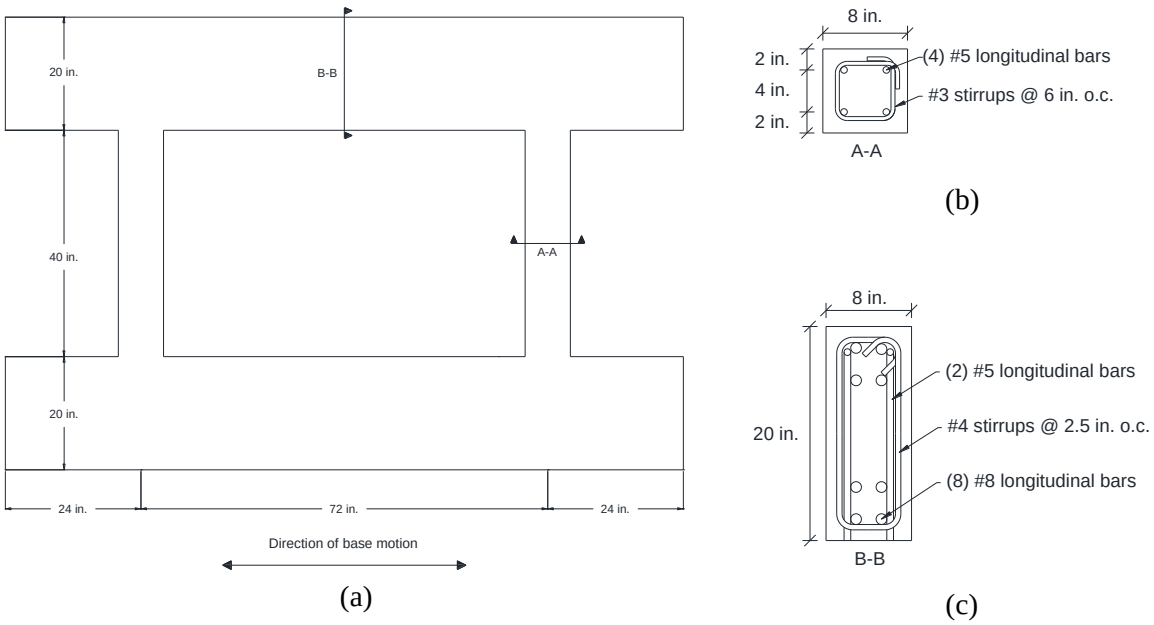

Fig. 3 – (a) Dimensions of frame, (b) Typical column cross-section, (c) Typical beam cross-section

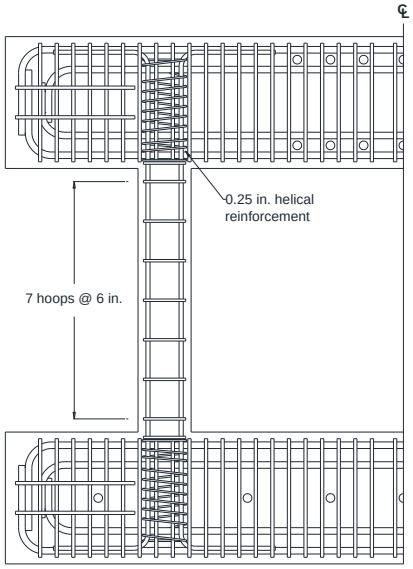

Fig. 4 – Reinforcement details

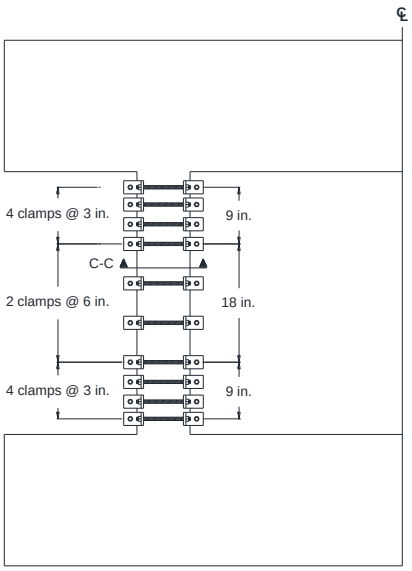

Fig. 5 – Clamp layout

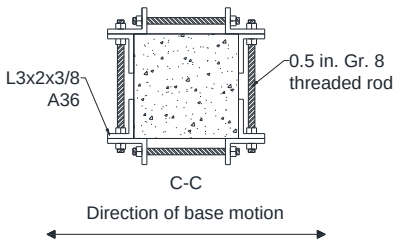

Fig. 6 – Typical clamp assembly

3. Observations

3.1 Series one: bare frame

Measurements from runs of the bare frame are shown in Table 1. Inclined cracks were first observed after the frame became nonlinear in Run 8 (40% - 1). The inclined cracks continued to increase with larger intensity ground motions. The maximum permanent crack width after Run 13 (80% - 2) was measured to be 0.075 in. Crack maps of the south column obtained after the second run at each intensity are shown in Fig. 7. North and south columns had similar crack patterns.

The variation of peak force (obtained from the load cell) with peak cumulative drift ratio is shown in Fig. 8. The peak cumulative drift ratio is the maximum drift measured in a run relative to the initial, undeformed position. The points in Fig. 8 can be considered to be an envelope for the force-displacement relationship of the bare frame.

The frame reached its lateral strength in Run 8 (40% - 1). The lateral strength of the bare frame was measured to be 24 kip, resulting in a base shear strength of approximately 50% of the weight of the structure (45 kip). In runs following Run 8, the maximum lateral force of the system was limited by the flexural capacity of the columns. Even though no shear failure was observed during the 80% runs (Runs 12 and 13), the size of the inclined cracks suggested it was likely that a shear failure may occur at a larger intensity run. Therefore, the bare frame was not subjected to the 100% motion.

Series one was completed with two additional repetitions at the 40% motion. Although the measured peak cumulative drift ratios between the first two and last two runs at the 40% motion differed by approximately 40% as a consequence of residual drift, the in-run drift ratios (the maximum drift measured during a run relative to the initial position at the beginning of the same run) between the two sets of runs differed by less than 20%. Given the scatter of the data this observation suggested that previous loading history did not affect the in-run drift demands in a critical manner. The difference in cumulative drift was mainly caused by permanent drift occurring in previous large-intensity runs. This observation is interesting because permanent drift is unlikely to affect repairs done after a large earthquake. The implication is that a structure repaired after an earthquake is not necessarily more vulnerable to a future ground motion than a new structure, for ground motion intensities strong enough to cause cracking and within conditions similar to those studied in this investigation.

3.2 Series two: frame with clamps

Measurements from runs of the frame with clamps are shown in Table 2. Before testing the frame with clamps, the maximum permanent crack width of the inclined crack at the top of the North column reduced from 0.075 in. to 0.02 in. after the final clamp was installed (Fig. 9). During runs of the frame with clamps, no additional inclined cracks formed. The widths of existing inclined cracks did not increase by more than 0.01 in. Additional flexural cracks formed with widths not larger than 0.02 in.

Fig. 8 shows the variation of peak force with peak cumulative drift ratio of the frame with clamps. Cumulative drift was calculated with respect to the position of the frame after installation of clamps. Drift was offset to reflect the idea that repairs are more likely to be sensitive to additional drift rather than prior permanent drift. The points in Fig. 8 represent an envelope for the force-displacement relationship of the frame with clamps. It was observed that the effective lateral stiffness of the frame with clamps was smaller than that of the bare frame. This was expected because of the effects of cracking and yielding of columns in series one. The maximum lateral force measured in runs of the frame with clamps was 23 kip and within 5% of that of the bare frame. Unlike the bare frame, the frame with clamps was subjected to the 100% motion. The confinement provided by the clamps maintained the integrity of the columns allowing for the frame to reach its lateral strength at a larger drift demand.

In series two, the frame with clamps was subjected to 12 runs of increasing intensities followed by 10 runs of decreasing intensities. The measured in-run drifts for ascending and descending runs of the same

intensity did not differ by more than 10%. This was similar to the displacement response of the bare frame and again suggested that previous loading history did not affect in-run drift demands in a critical manner.

4. Results

To explore the correlation of peak in-run and cumulative drifts and ground motion parameters, the variation of drift with PGV and PGA is shown in Fig. 10 and 11. Based on these figures, it was concluded that PGV helped organize peak drift measurements better than PGA, and drift and PGV had a nearly linear relationship. Values of PGA were found to be sensitive to filtering methods. The nearly linear variation of drift and PGV is similar to results observed by Sozen from dynamic tests of three-story reinforced concrete frames [6, 7].

Fig. 12 shows the displacement histories of the bare frame and frame with clamps. In both series of tests, the peak in-run and cumulative drifts of the ascending portion were similar to those of the descending portion for the same series at the same intensities. The maximum difference was approximately 20% for in-run drifts and 40% for cumulative drifts. This suggests that (1) previous loading history does not affect the drift demand of a regular frame given there is no localized failure, and (2) lower intensity runs after a large-intensity run cause similar drift demands as that of a single low-intensity motion. An obvious exception to this second observation is that of a motion not intense enough to cause cracking in a pristine structure. These observations are consistent with observations made by Cecen and Laughery [8, 9].

Comparing the bare frame with the frame with clamps, both peak in-run and cumulative drift demands at the same intensities did not differ by more than 25% for all runs except for the 10% motion. For the 10% motion in series one the frame was uncracked but in series two the frame was cracked. This resulted in a difference in drift demands that were almost twice as large in series two in comparison to series one.

The frame with clamps was subjected to the 100% motion to investigate the effects of the clamps on strength, drift demand, and toughness. At this intensity, the frame with clamps reached the same lateral strength as series one at a larger drift demand. This is because the addition of clamps maintained the integrity of the columns and reduced the maximum crack widths of inclined cracks. Similar observations were made by Skillen where columns with clamps had larger drift capacities than similar columns without clamps. Although the bare frame was not tested to failure, the tests showed that the toughness provided through the addition of clamps can be remarkable, with the repaired frame sustaining 22 demanding motions without a loss of strength.

In series one, the maximum permanent offset was measured to be approximately 0.25 in. In series two, the maximum permanent offset relative to the initial position of the frame after the clamps were installed was half of that in series one. This was deemed to be a consequence of confinement provided by adding clamps.

5. Future Work

As masonry construction materials are readily available and inexpensive in many seismic regions, masonry infill walls seem to be a practical solution for stiffening vulnerable buildings. A masonry infill wall will be added to the damaged frame with clamps for a third series of tests. The addition of the infill wall is expected to add lateral stiffness to the system and decrease seismic drift demand. An assumption implicit in the upcoming test on the frame with infill wall is that out-of-plane failure does not precede in-plane failure. The peak in-run drifts of the frame are expected to be a small percentage, perhaps less than 25% of the bare frame and frame with clamps.

6. Conclusion

1. Drift was observed to increase in nearly linear fashion with PGV. This trend was especially clear when drift was offset to exclude permanent (or residual) displacements from previous runs.
2. Drift (relative to the initial position in each simulation) was observed to be nearly insensitive to previous damage (that did not include local failure) except in the extreme case in which comparisons

were made between the pristine specimen and the specimen after cracking for simulations with small intensities (10% motion). For moderate and large-intensity simulations, drift relative to the geometry of the pristine structure (cumulative drift) was also observed to be nearly insensitive to previous damage.

3. Clamps were used to repair columns that were judged to have been close to shear failure. The clamps were post-tensioned to produce an initial transverse prestress comparable to the peak nominal shear stress expected in each column. The repaired frame sustained 22 demanding motions without exhibiting perceptible signs indicating reduction in resistance to seismic demands.

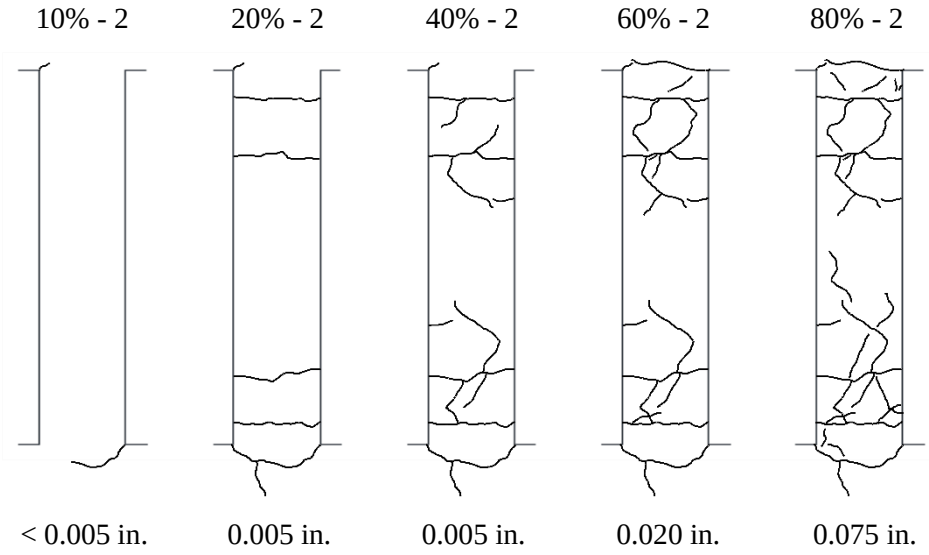

Fig. 7 – Crack maps of east face of south column in series one

Note: Values below crack maps are measured maximum permanent crack widths after the indicated runs

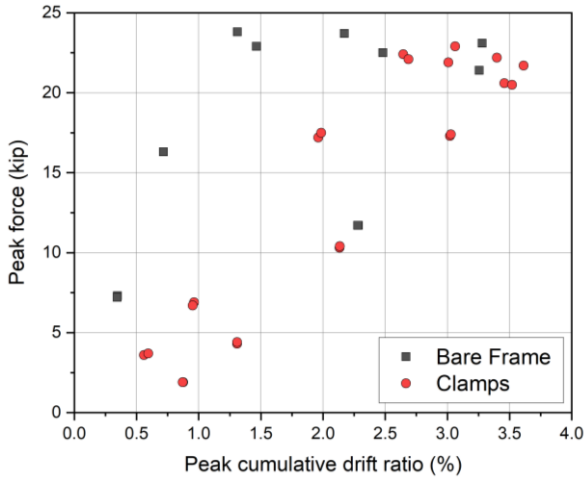

Fig. 8 – Peak force vs. peak cumulative drift ratio for all test runs

Table 1 – Test summary for bare frame

Run	Intensity	PGA (g)	PGV** (in/s)	PGD** (in)	Peak force (kip)	Peak cumulative drift (in)	Peak in-run drift (in)
1	10% -1*	0.4	1.6	0.16	7	0.06	0.06
2	10% -2*	0.4	1.8	0.16	7	0.07	0.07
3	10% -3*	0.4	1.7	0.16	8	0.08	0.07
4	20% -1*	0.8	3.3	0.32	13	0.18	0.17
5	10% - 4	0.6	1.7	0.16	7	0.14	0.12
6	10% - 5	0.6	1.6	0.16	7	0.14	0.12
7	20% - 2	0.8	3.0	0.32	16	0.29	0.28
8	40% - 1	1.0	5.0	0.64	24	0.53	0.54
9	40% - 2	0.7	4.7	0.64	23	0.59	0.59
10	60% - 1	1.0	6.8	0.96	24	0.87	0.83
11	60% - 2	1.1	6.6	0.96	23	0.99	0.95
12	80% - 1	0.9	8.2	1.3	23	1.3	1.3
13	80% - 2	1.2	8.1	1.3	21	1.3	1.1
14	40% - 3	0.6	4.9	0.64	12	0.91	0.68
15	40% - 4	0.7	5.2	0.64	12	0.91	0.68

*Swivel without mechanical fasteners

**Values of PGV and PGD were inferred from values of measured base accelerations

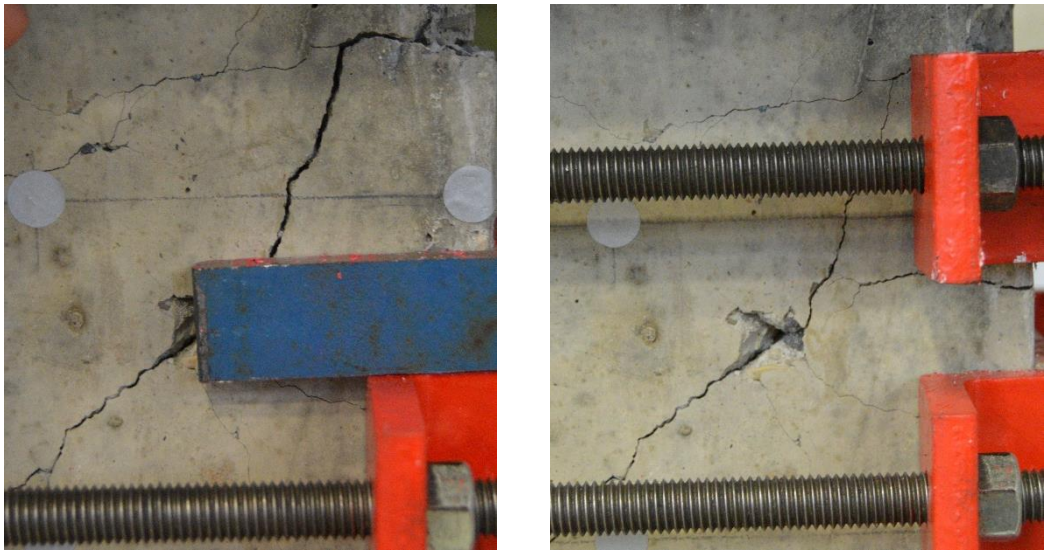

(a) (b)

Fig. 9 – Top of north column, west face (a) before and (b) after final clamp was installed

Table 2 – Test summary for frame with clamps

Run	Intensity	PGA (g)	PGV** (in/s)	PGD** (in)	Peak force (kip)	Peak cumulative drift (in)	Peak in-run drift (in)
16	10% - 1	0.4	1.6	0.16	4	0.22	0.23
17	10% - 2	0.4	1.4	0.16	4	0.24	0.23
18	20% - 1	0.6	2.9	0.32	7	0.39	0.37
19	20% - 2	0.6	2.9	0.32	7	0.38	0.36
20	40% - 1	0.8	5	0.64	17	0.79	0.76
21	40% - 2	0.8	5.1	0.64	18	0.79	0.78
22	60% - 1	0.8	7.1	0.96	22	1.1	1.0
23	60% - 2	0.7	7.1	0.96	22	1.1	1.1
24	80% - 1	0.8	8.5	1.3	23	1.2	1.2
25	80% - 2	0.9	8.6	1.3	22	1.2	1.2
26	100% - 1	1.0	10.5	1.6	22	1.4	1.4
27	100% - 2	1.0	10.4	1.6	22	1.5	1.5
28	80% - 3	0.9	8.4	1.3	21	1.4	1.3
29	80% - 4	0.9	8.2	1.3	21	1.4	1.3
30	60% - 3	0.8	7.1	0.96	17	1.2	1.1
31	60% - 4	0.8	7	0.96	17	1.2	1.1
32	40% - 3	0.6	4.5	0.64	10	0.85	0.72
33	40% - 4	0.6	4.5	0.64	10	0.85	0.72
34	20% - 3	0.5	2.9	0.32	4	0.52	0.39
35	20% - 4	0.5	2.9	0.32	4	0.52	0.39
36	10% - 3	0.3	1.3	0.16	2	0.35	0.22
37	10% - 4	0.3	1.2	0.16	2	0.35	0.22

**Values of PGV and PGD were inferred from values of measured base accelerations

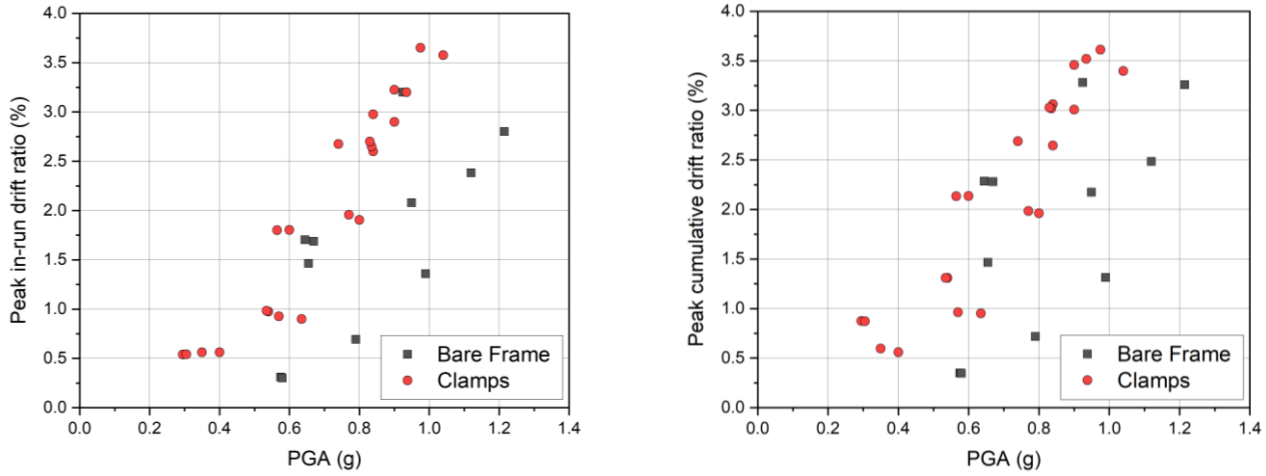

(a) (b)

Fig. 10 – (a) Peak in-run drift ratio vs. PGA, (b) Peak cumulative drift ratio vs. PGA

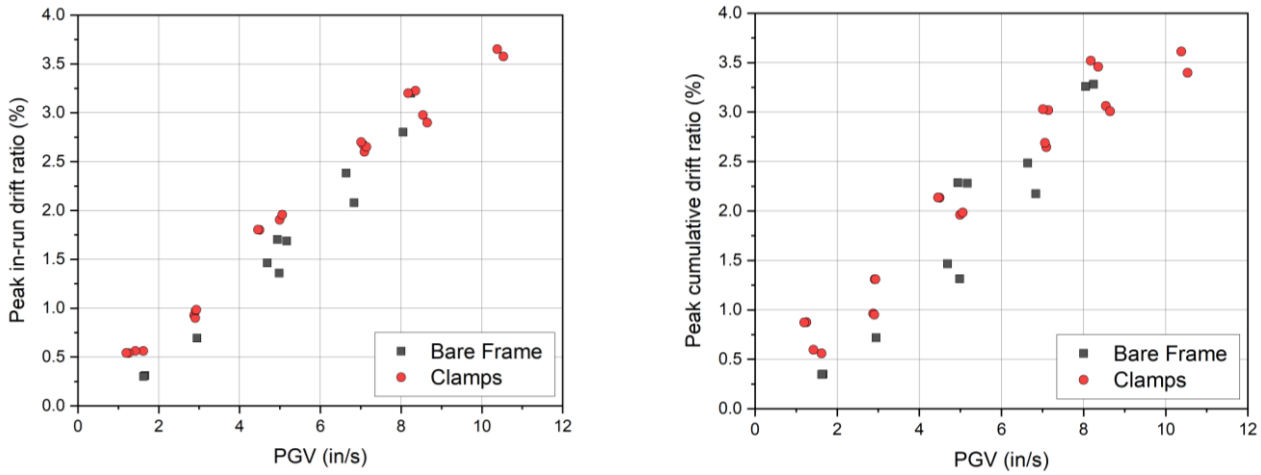

(a) (b)

Fig. 11 – (a) Peak in-run drift ratio vs. PGV, (b) Peak cumulative drift ratio vs. PGV

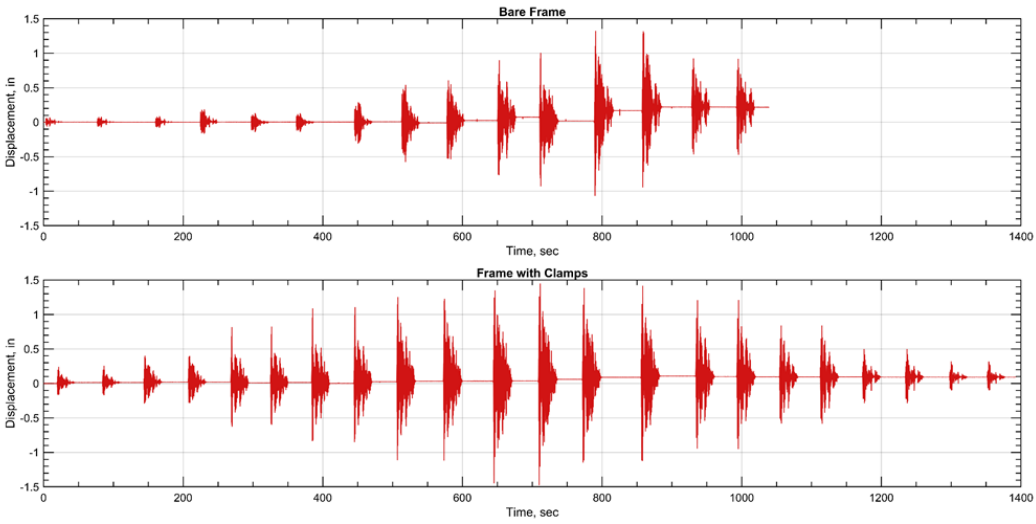

Fig. 12 – Cumulative displacement history for all test runs

7. Acknowledgements

The help of fellow graduate students and lab technicians at Bowen Laboratory at Purdue University is greatly appreciated.

8. Copyrights

9. References

[1] Skillen, K. (2020): An experimental study of the bond and shear behavior of reinforced concrete with lateral confinement. *Unpublished PhD Dissertation.* Purdue University, West Lafayette, IN, USA.

[2] Sezen, H. (2002): Seismic behavior and modeling of reinforced concrete building columns. *PhD Dissertation.* University of California at Berkeley, Berkeley, CA, USA.

[3] Yamakawa, T., Kamogawa, S., Kurashige, M. (2000): Seismic performance and design of RC columns retrofitted by PC bar prestressing as external hoops. *Journal of Construction Engineering*, AIJ, Japan, No. 537, pp.107-113.

[4] Sozen, M., Otani, S., Gulkan, P., Nielsen, N. (1969): The University of Illinois earthquake simulator. Proceedings, Fourth World Conference on Earthquake Engineering, Santiago, Chile, Vol. 3, pp.139–150.

[5] Chiou et al. (2008): NGA project strong-motion database. *Earthquake Spectra*, Vol. 24, No. 1. pp. 23-44.

[6] Sozen, M. (2013): Why should drift drive design for earthquake resistance? Proceeding the 6th Civil Engineering Conference in Asia Region: Embracing the Future through Sustainability, Jakarta, Indonesia.

[7] Otani, S., Sozen, M. (1972): Behavior of multistory reinforced concrete frames during earthquakes. *Civil Engineering Studies, Structural Research Series*, University of Illinois at Urbana-Champaign, Urbana, IL, USA. Vol. 392. 551 pp.

[8] Cecen, H. (1979): Response of ten story, reinforced concrete model frames to simulated earthquakes. *PhD Dissertation*, University of Illinois at Urbana-Champaign, Urbana, IL, USA. 352 pp.

[9] Laughery, L. (2016): Response of high-strength steel reinforced concrete structures to simulated earthquakes. *PhD Dissertation.* Purdue University, IN, USA. 320 pp.

